STUDIES OF FAST WIRE SCANNERS FOR LEP

C. Fischer, G. Burtin, R. Colchester, B. Halvarsson, R. Jung, J.M. Vouillot
European Organization for Nuclear Research (CERN)
CH-1211 Geneva 23, Switzerland

Abstract : Fast wire scanners were developed to measure the transverse density distributions of LEP bunches. Secondary emission will provide the profile of the beam core. Bremsstrahlung emission resulting from the beam-wire interaction will permit investigation of very low density tails. Monitors will be installed at dispersion-free locations and will provide an absolute measurement of beam dimensions. Tests of a mechanical prototype have shown that the required speed and resolution can be achieved

1. Introduction

With respect to synchrotron light monitors, detectors based on the displacement of a wire through the beam give substantial advantages. They can be installed in straight sections at dispersion-free locations, hence providing beam dimensions resulting from the transverse phase space distributions only.

2. Beam and Machine Requirements

Taking the nominal transverse emittance ratio of 25 in LEP, a high β_V location will equalize the beam distributions between the H and V planes. If measurements are to be performed on each individual bunch, sufficient time ($\Delta t > 1$ μs) must be allowed between the passage of two bunches. By locating the monitor in a straight section one avoids beam dispersion and problems from synchrotron radiation. The chosen position in LSS1 will allow Bremsstrahlung emission to leave the vacuum pipe by the window already foreseen for the LEP polarimeter [1], with resulting parameters : $\Delta t = 1.5$ μs, $\beta_H = 13.1$ m, $\sigma_H = 0.85$ mm, $\beta_V = 79.8$ m, $\sigma_V = 0.42$ mm.

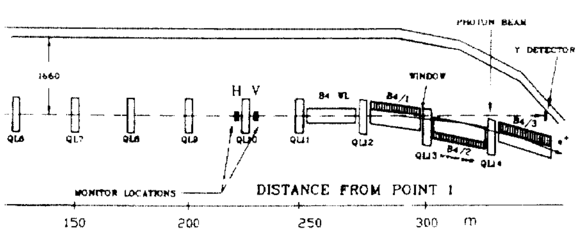

Fig. 1 General layout

The scanning speed and wire diameter are a compromise between precision and parasitic effects. With the LEP revolution period $T = 88.9$ μs, a sweeping speed v of 1 m/s will provide 10 points per σ_H and 5 points per σ_V. Light materials will minimize the interaction between the wire and the beam. A wire with a diameter d of 20 μm will provide sufficient resolution. Wire scanners with 36 μm carbon wire are widely used at CERN [2].

3. Parasitic Effects

3.1 Wire Heating

The energy lost for N particles by atomic electron collisions within the wire is :

$$\Delta E = N\ dE/dx\ \pi d^2/4vT$$

with $N = 3.2 \times 10^{12}$, $dE/dx = 8.36$ MeV/cm.
The wire mass heated during a horizontal scan is :

$$M = \pi d^2/4\ h_{eff}\ \rho\ (\text{with } h_{eff} = \sqrt{2\pi}\sigma_V)$$

The temperature rise after one complete scan is therefore $\Delta T = 1420$°K. This has to be compared to the carbon fusion point of 3700°C. In fact, part of the atomic electrons released leave the wire and only a fraction of ΔE evaluated at 25 % to 30 % contributes to the wire heating [2].

3.2 Beam Blow-up and Beam Losses

Multiple Coulomb scattering of the beam through the carbon wire will, on average, increase both emittances $\varepsilon_{H,V}$ by :

$$\Delta\varepsilon_{H,V} = \beta_{H,V} <\theta^2>$$

where $<\theta^2> = 0.26$ μrad^2 is the average square scattering angle; hence the emittance increase will be below 1 % per scan.

Incident particles traversing the wire will loose energy by radiation (Bremsstrahlung). If the loss is large, they will escape the RF bucket. The probability for a particle to emit a photon of energy $E_\gamma > E$ through a material thickness x is :

$$P(E<E_\gamma<E_o) = \frac{x}{L_R} \int_E^{E_o} \frac{dE_\gamma}{E_\gamma} \quad (1)$$

where $E_o = 55$ GeV. The LEP nominal bucket height being ± 275 MeV and assuming that a particle loosing more than $\Delta E = 135$ MeV is lost, then the relative loss $\Delta N/N$ per scan is :

$$P(\Delta E < E < E_o) = 1.1 \times 10^{-4}.$$

As these disturbances looked acceptable, a system based on the parameters quoted above has been developed.

4. Achievements

The design goal was to achieve a wire speed of 2 m/s over a beam scanning area of 20 mm x 20 mm, with position resolution of better than 20 μm, good radiation resistance, low higher order mode losses of the vacuum enclosure and low cost. No existing design was available which satisfied all these requirements simultaneously.

Good radiation resistance plus excellent position information had already been achieved with previous wire scanners driven by stepping motors [5]. A stepping motor allows precise static positioning of a wire as well as high speed scanning. To achieve the best angular resolution, motors with 500 steps per turn have been controled with interpolated steps. Step interpolation has the advantage of providing higher rotational speeds with a smoother movement which in turn decreases the risk of wire oscillations.

The monitor design was of the oscillating arm type. The dimensions of the arm were a compromise of several factors : rigidity, low inertia transferred back to the motor shaft, wire speed and vacuum tank dimensions. The resulting arm was made of 2.5 mm thick Titanium with a length of 210 mm and a height ranging from 22 to 5 mm (Fig. 2). The arms yield sufficiently along the wire direction to give the desired tension of 25 grams on the 40 mm long carbon wire. The fundamental vibration frequency of the wire in this arrangement is 4 kHz. The stepping motor had a torque of 0.7 Nm. The coupling between the motor shaft and the rotation axis of the support arm was through a 0.1 mm thick titanium band and a 0.3 gear ratio. The drive electronics was similar to the one

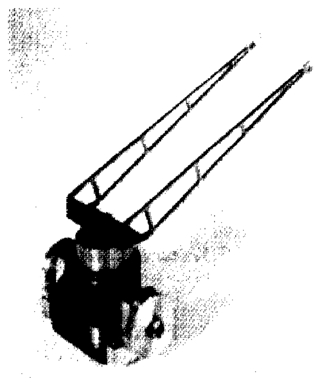

Fig. 2 Wire supporting arms with bellows

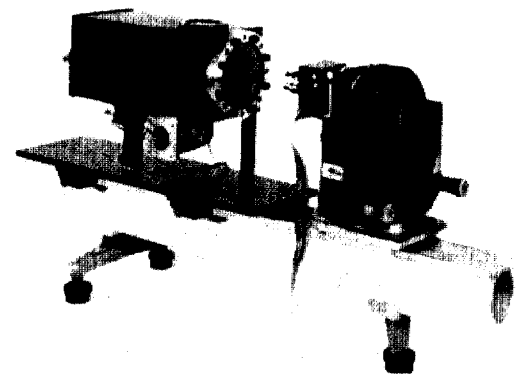

Fig. 4 Test set-up showing the wire scanner tank and the CCD camera head

described in [5]. It is of the DC bipolar type giving 32000 interpolated steps per turn. The drive electronics block diagram is shown in Fig. 3.

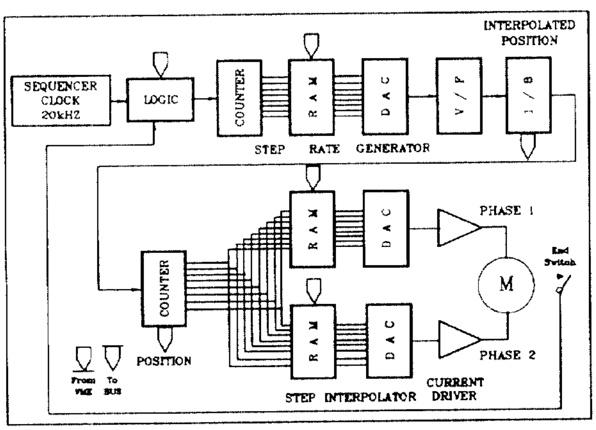

Fig. 3 Wire scanner drive electronics

The control electronics were in the VME standard. The scanning cycle is generated by a sequencer having an internal 20 kHz clock. The parameters of the sequence: acceleration, speed, and shape of the motor phases are preset in RAM by the VME crate controller. This set-up gave an incremental resolution of 14 µm. By dividing down by 8 the V/F generated step frequency, an interpolated resolution of 1.75 µm can be obtained. The step frequency is swept from 600 Hz to 150 kHz and back in 60 ms at an average rate of 30 Hz/µs, resulting in extremely low energy available to drive vibrations in the wire.

A static evaluation of the precision obtained with interpolated steps showed that it was necessary to adjust separately the amplitudes of the driving phases. The result of this adjustment was a non linearity of ± 1 ministep, i.e. ± 14 µm, with a period of approximately 4 full steps. The measurements were at the limit of the resolution of the measuring set-up. The effect of this non-linearity on the fit has been checked with a peak to peak amplitude of 60 µm. The error on the rms value of the distribution is smaller than 1.3 %. The maximum speed obtained under vacuum was 2.4 m/s. There is no significant gain of precision when going from a speed of 2 m/s (2.5 points/σ_y) to 1 m/s. The dynamic test was more difficult. We chose to make use of a development made for the synchrotron light monitor for LEP which uses a digitized profile capture system based on a CCD TV camera chip. The illumination consisted of a light pulse of 1 µs FWHM, which resulted in a smearing of less than 2 µm of the wire. The test set-up without the light source is shown in Fig. 4. By delaying the light pulse it was possible to verify the precision of the displacement. Investigation of the wire oscillations were all done with the system under vacuum. The 36 µm wire was imaged onto one CCD pixel row which gave an observable wire length of 384 x 36 µm = 14 mm. The data was processed by calculating the vertical center of charge of the CCD columns. Under these conditions, one arrives at a vertical resolution of better than 10 µm. Wire profiles obtained at rest and under movement were compared. No deformation was observed within the available resolution. To make sure that vibrations would be detectable, we deliberately tried to vibrate the wire during a normal sweep. This proved quite difficult. We eventually provoked and observed oscillations by reducing the amplitude of one of the motor phases. The test results are shown in Fig. 5. The deformation looks like a 2nd harmonic oscillation with an amplitude of about 50 µm.

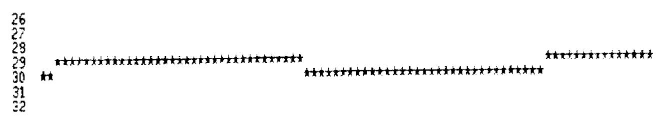

Static and moving wire at 2 m/s (normal phases)

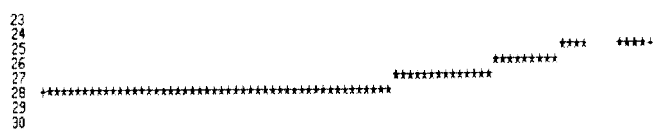

Moving wire at 2 m/s (unbalanced phases: 30 %, 100 %)
Horizontal: 12 mm full scale, vertical: 9 µm/line.

Fig. 5 Test results: high resolution scan

We also observed the whole length of the wire but this reduced the CCD raw resolution to 100 µm. For usable results we had to subtract a reference frame taken under the same light conditions as for the moving wire. The same measurements as before were taken, they confirmed our previous results.

Static and moving wire at 2 m/s (normal phases)

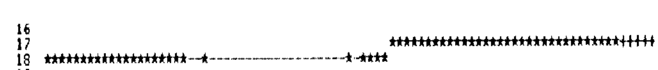

Moving wire at 2 m/s (unbalanced phases).
Horizontal: 34 mm full scale, vertical: 25 µm/line.

Fig. 6 Test results: low resolution scan

Work is under way to modify the design of [2] to bring it closer to our requirements. This would result in a common instrument in both LEP and SPS machines.

5. Monitored Signals

5.1 Secondary Emission

By collecting the charges released from the wire at each traversal of the beam one can get a transverse profile. Assuming an efficiency η of 5×10^{-2} the charge collected per traversal is :

$$Q = e \eta \, dN/dy \, d$$

with dN/dy the bunch density. The signal at the distribution center is then respectively 30 pC and 60 pC for the H and V-planes. With an expected electronic sensitivity of 0.1 pC, tails down to 10^{-2} of the maximum density could be investigated; The interval between bunch passages being always more than 1.5 µs should allow simultaneous recording of profiles of all eight bunches with the same device.

5.2 Bremsstrahlung Emission

The number of photons and the energy produced per traversal can be calculated with Eq. (1) [3].

$$N_\gamma = \pi d^2/4L_R \, dN/dy \, \ell_n(E_o/E_{min})$$

$$W_\gamma = \pi d^2/4L_R \, dN/dy \, (E_o - E_{min})$$

Table 1 gives the expected signal at the distribution center for various values of E_{min}.

T A B L E 1

	H-plane			V-plane		
E_{min}(GeV)	10^{-3}	1	10	10^{-3}	1	10
$N_\gamma(10^6)$	3.5	1.3	0.6	7.1	2.7	1.1
$W_\gamma(10^7$GeV)	1.79	1.76	1.47	3.6	3.55	2.97

The low energy part of the spectrum contributes only a little to the total emitted energy.

5.2.1 Background Sources : Bremsstrahlung photons leave the vacuum chamber through a window at about 80 m from the monitors (Fig. 1). This window sees the 500 m straight section where the monitors are installed and two possible background sources need to be considered :

- Synchrotron radiation from correction dipoles : if all 16 dipoles are powered at 25 %, they will produce photons above 0.5 MeV with an energy five orders of magnitude lower than the Bremsstrahlung emission at the center of the distribution.
- Beam-gas Bremsstrahlung : photons will also be produced from the interaction of the beam with the residual gas atoms, along the length L of the straight section; the ratio between the real signal at the beam center and this noise is :

$$R = \frac{dN/dy \; d \; \pi/4 \; d/L_{R(wire)}}{N_{bunch} \; L/L_{R(N_2)}}$$

With $N_{bunch} = 4.1 \times 10^{11}$ particles and a N_2 equivalent pressure of 3×10^{-9} Torr, we get $R \simeq 7 \times 10^4$, assuming that all beam-gas photons reach the detector. The signal-to-noise ratio therefore allows scanning of the tails over 5 orders of magnitude.

5.2.2 Extracted signal : The window, located at 78.59 m and 74.57 m from the H and V-monitors (Fig. 1) has finite dimensions (± 23 mm horizontally and ± 9 mm vertically) with respect to the straight section axis and defines the detection acceptance. Photons produced in the wire have a phase space distribution given by a convolution of the beam divergence with their average emission angle $<\theta_\gamma>$;
at a given position y(x or z) if the beam divergence is $\sigma_{y'} = \sqrt{\epsilon_y/\beta_y}$, the photon beam divergence $\tilde{\sigma}_{y'}$ is :

$$\tilde{\sigma}^2_{y'} = \sigma^2_{y'} + <\theta^2_\gamma>$$

$$\text{with } <\theta^2_\gamma> = \frac{1}{\sqrt{2}} \, q(E_o, E_\gamma, Z) \, \frac{mc^2}{E_o} \, \ell_n \left(\frac{E_o}{mc^2}\right)$$

mc^2 being the electron rest mass and $q \simeq 0.7$. In the photon transverse phase plane the window acts as an aperture limit represented by the lines :

$$x + 78.59 \, x' = \pm 23 \quad \text{H-plane}$$
$$z + 74.57 \, z' = \pm \; 9 \quad \text{V-plane}$$

For a transverse position y (x or z), only a fraction f of the produced signal passes the window acceptance; f_y has been evaluated in [3] for various values of y: Table 2. The effect is more pronounced in the V-plane up to 8 σ_y where 80 % of the signal still leaves the chamber.

T A B L E 2

x (mm)	fx (%)	z (mm)	fz (%)
8.5 = 10 σ_x	55.2	4.2 = 10 σ_z	74.3
4.25 = 5 σ_x	96.4	2.1 = 5 σ_z	92.6
1.7 = 2 σ_x	99.8	0.84 = 2 σ_z	96.9
0.85 = σ_x	99.9	0.42 = σ_z	97.4
0	99.95	0	97.6

5.2.3 Γ-Detector Requirements : Extracted photons will be analyzed by a detector located at 57 m from the window (Fig. 1). Silicon plates are being considered; test results [4] have shown that the deposited energy in a 300 µm thick Si-plate is of the order of 10^7 MeV at the bunch center. The low density tails can be investigated without difficulties because of the expected low background rate.

6. Conclusion

The sensitivity of the electronics used to measure the secondary emission will allow full beam profiles to be measured. The time interval between bunches is such that both beams can be analyzed in one sweep with the same device.

Bremsstrahlung emission provides a convenient way to analyze very low density tails even when seriously off-centered; the signal directivity imposes the use of one detector for each beam.

References

[1] M. Placidi, The Transverse Polarimeter for LEP, in Proceedings of this Conference.

[2] J. Bosser et al., The Micron-Wire Scanner at the SPS, CERN/SPS/86-26 (MS).

[3] C. Fischer, A Study of a wire scanner for LEP, LEP Note 563, 2nd June, 1986.

[4] J.Y. Hemery et al., An Interaction Rate Monitor for LEP, CERN/LEP-BI/86-5.

[5] R.J. Colchester et al., Position control in radiation environments, CERN/LEP-BI/86-08, 17.2.86.